



Synthesis and biochemical analysis of 2,2,3,3,4,4,5,5,6,6,7,7-dodecafluoro-N-hydroxy-octanediamides as inhibitors of human histone deacetylases

Leonhard M. Henkes^a, Patricia Haus^a, Felix Jäger^b, Joachim Ludwig^b, Franz-Josef Meyer-Almes^{a,*}

^aDepartment of Chemical Engineering and Biotechnology, University of Applied Sciences, Schnittspahnstraße 12, 64287 Darmstadt, Germany

^bSynchem OHG, Am Kies 2, 34587 Felsberg/Altenburg, Germany

ARTICLE INFO

Article history:

Received 22 September 2011

Revised 15 November 2011

Accepted 20 November 2011

Available online 30 November 2011

Keywords:

Histone deacetylase

Histone deacetylase inhibitors

SAHA

Vorinostat

Oncology

ABSTRACT

Inhibition of human histone deacetylases (HDACs) has emerged as a novel concept in the chemotherapeutic treatment of cancer. Two chemical entities, SAHA (ZOLINZA, Merck) and romidepsin (Istodax, Celgene) have been recently approved by the FDA as first-in-class drugs against cutaneous T-cell lymphoma. Clinical use of these drugs revealed several side effects including gastro-intestinal symptoms, fatigue, thrombocytopenia, thrombosis. Romidepsin is associated with an yet unresolved cardiotoxicity issue. A general hypothesis for the diminishment of unwanted adverse effects and an improved therapeutical window suggests the development of more isotype selective inhibitors. In this study the first time HDAC inhibitors with perfluorinated spacers between the zinc chelating moiety and the aromatic capping group were synthesized and tested against representatives of HDAC classes I, IIa and IIb. Competitive binding assays and a combined approach by using blind docking and molecular dynamics support binding of the perfluorinated analogs of SAHA to the active site of the HDAC-like amidohydrolase from *Bordetella/Alcaligenes* and presumably also to human HDACs. In contrast to the alkyl spacer of SAHA and derivatives, the perfluorinated alkyl spacer seems to contribute to or facilitate the induction of selectivity for class II, particularly class IIa, HDACs even though the overall potency of the perfluorinated SAHA analogs in this study against human HDACs remained still rather moderate in the micromolar range.

© 2011 Elsevier Ltd. All rights reserved.

1. Introduction

The interaction between histone octamers and nuclear DNA depends on the acetylation state of their N-terminal lysine residues. By binding tightly to the DNA backbone, deacetylated lysine residues suppress the process of transcription, while acetylated lysine residues support a further relaxed state, associated with increased transcription rates.¹ The process of deacetylation is catalyzed by a group of proteins, the so called histone deacetylases (HDACs). In contrast, histone acetyltransferases (HAT) reverse this process antagonistically. HDACs are divided into four different classes (I, II, III and IV) depending on their yeast homologs RPD3, HDA1 and Sir2.^{2,3} The classic HDACs share a coordinated Zn²⁺ ion in their active site and comprise members of class I (HDACs 1, 2, 3 and 8), class II (HDACs 4, 5, 6, 7, 9, 10) and class IV (HDAC11). Class II can be subdivided into the nucleus–cytosol shuttling class IIa HDACs 4, 5, 7, 9 and the mainly cytoplasmic class IIb HDACs HDAC6 and HDAC10, which possess two catalytic domains.⁴ Class III members, the so called sirtuins, are distinguished from the classic HDACs by their NAD⁺ dependent hydrolytic activity.² In the cytosol class II HDACs are involved in posttranslational modifications and pro-

cess non histone substrates.⁵ Due to their nuclear and cytosolic presence, HDACs impact many fundamental cellular functions, including oncogenic and apoptotic pathways.⁶ In particular, different HDAC isoforms contribute to numerous cell and tissue specific processes during cancer induction and growth. The catalytic domain of Zn²⁺ containing HDACs is highly conserved and consists of a tunnel leading to a buried Zn²⁺ ion within the active site, that coordinates the substrate and a hydrolytic water molecule.⁷ The reaction mechanism for classes I and IIb HDACs is supposed to be mediated through a histidine–aspartate charge-relay system which increases the nucleophilic character of a Zn²⁺ coordinated water molecule thereby enabling its nucleophilic attack on the carbonyl carbon atom of the substrate. The resulting intermediate is stabilized by an adjacent tyrosine residue. Then the carbon–nitrogen bond is cleaved supported by a second charge-relay system finally resulting in an acetate molecule and a deacetylated lysine residue. Common histone deacetylase inhibitors (HDACi) sharing the zinc chelating hydroxamate group like suberoylanilide hydroxamic acid (SAHA) and Trichostatin A (TSA) intervene substrate deacetylation by forming chelate complexes with the catalytic Zn²⁺ ion. SAHA and TSA have been shown to interfere with cell growth and prevent tumor differentiation in mice.⁶ However, treatment of cancer patients with SAHA is accompanied with several side effects which may result from poor isoform selectivity.

* Corresponding author. Tel.: +49 (0) 6151168406; fax: +49 (0) 6151168404.

E-mail address: franz-josef.meyer-almes@h-da.de (F.-J. Meyer-Almes).

This vindicates a strong demand for new chemical entities exhibiting optimized HDAC isoform selectivity profiles.⁶ All HDACi of the hydroxamic acid type consist structurally of a cap moiety attached to a mostly aliphatic carbon linker and a zinc binding group (e.g., hydroxamic acid moiety) at the opposing side of the linker. In the attempt to synthesize new HDACi's, the zinc binding groups and different capping structures have been extensively varied, while the spacer was almost exclusively an alkyl chain of different length.⁸ Though the importance of the linker component of HDACi's has been recognized recently^{9,10}, the chemistry of spacers has just been varied sparsely. This inspired us to substitute the suberoyl linker of SAHA by a perfluorinated analog and to analyze the effect on inhibitory activity and selectivity. Compounds with perfluorinated alkyl spacer turned out to be inhibitors of HDAC-like amidohydrolase (HDAH) from *Bordetella*¹¹ with similar IC₅₀ values as SAHA. To further explore the effect of hydroxamic acids with perfluorinated alkyl spacer on human HDACs and to possibly induce distinct isoform selectivity, a series of analogs with different aromatic and heteroaromatic capping groups was synthesized and tested against a panel of representative recombinant human classes I, IIa and IIb HDACs and lysates of human K562 cells.

2. Results

2.1. Chemistry

The reported standard synthesis of SAHA¹² via the formation of a cyclic anhydride did not work with dodecafluorooctanedioic acid, probably due to the high electronegativity of the fluorine atoms. Instead of the anhydride the acid dichloride **2** was synthesized. Another modification to the SAHA synthesis applied to the intermediate synthesis of the benzylester **3** which served as chemical starting point for the synthesis of all perfluorinated compounds (see Scheme 1). One of the chlorides of 2,2,3,3,4,4,5,5,6,6,7,7-dodecafluorooctanedioyldichloride **2** was substituted by benzyl alcohol, leading to benzyl-7-chlorocarbonyl-2,2,3,3,4,4,5,5,6,6,7,7-dodecafluoroheptanoate **3**. For the introduction of several new cap groups the obtained benzyl 7-chlorocarbonyl-2,2,3,3,4,4,5,5,6,6,7,7-dodecafluoroheptanoate was reacted with different aromatic amines in the presence of a base. The base may be an inorganic or organic base like sodium carbonate, triethylamine or pyridine. The hydroxamic acid function is introduced by a final reaction with hydroxylamine in form of its inorganic salt, aqueous solution in THF or any miscible solvent yielding the desired hydroxamic acid.

Perfluorinated hydroxamic acids were divided into four main groups due to the chemical structure of the capping group. The Aniline like cap structures **4–10** and **12** represent the largest group of our set. To analyze the positional effect of the perfluorinated

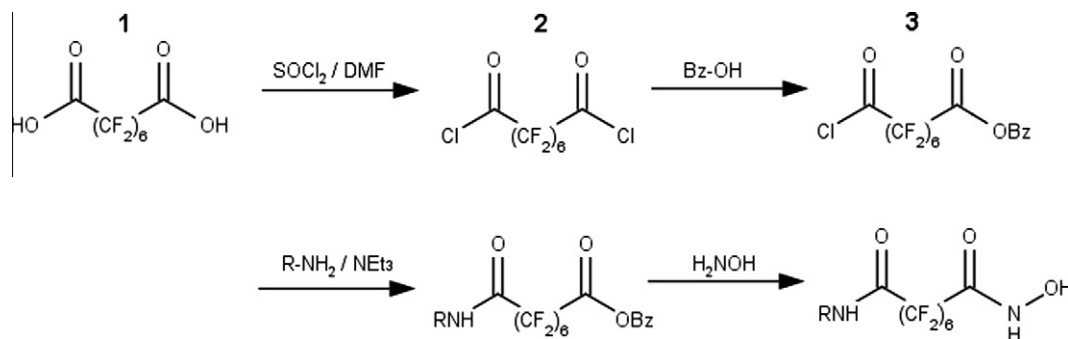
spacer with hydroxamic acid function at the capping group on enzyme inhibition, biphenyl derivatives **11**, **18** and **20** were synthesized as well. Based on their strong similarities to the potent HDACi SAHA, these were the first structures we started with. To further evaluate the sterical influence of the capping group on the inhibitory potency and selectivity, we synthesized perfluorinated analogs with aromatic capping groups of different sizes (**17**, **19**, **21**, **22**, **23**). In former studies, aromatic residues with a maximum of two rings were frequently used, while larger moieties remained uninspected.⁸ Heterocycles were already found to modulate the inhibitory potential in several SAHA analogs.⁸ Therefore, the triazole containing compounds **13** and **16** were synthesized. In contrast to these compounds, the thiazole heterocycle **15** was directly attached to the perfluorinated spacer. SAHA (**25**) was used as a general reference HDACi for all assays. To exclude unspecific contributions of the perfluorinated spacer to the observed interaction with HDAH and HDACs, compound **24** that lacked the zinc chelating hydroxamate group was used as a negative control compound.

2.2. Biochemical and biological characterization

In order to evaluate the inhibitory potential of the newly created perfluorinated compounds **4–24**, fluorogenic enzyme activity assays were conducted to obtain IC₅₀ values for different recombinant human HDAC isoforms and the bacterial HDAC homolog HDAH. The HDAC classes are represented by HDAC1, HDAC8 (class I), HDAC6 (class IIb) and HDAC7 (class IIa). While HDAC1 and HDAC8 are still members of the same class, they clearly differ in their selectivity for substrates and inhibitors.¹³ The competitive dual parameter binding assay was used to obtain more information about the binding site of the representative compound **4**. For further compound characterization cancer cell line experiments have been performed. All compounds of interest (IC₅₀ < 10 μM) were also tested in lysates of K562 cancer cells using the acetylated and trifluoroacetylated substrates Boc-L-Lys(Ac)-MCA and Boc-L-Lys(TFA)-MCA to measure the intrinsic HDAC activity of the K562 cells.

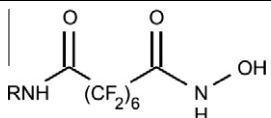
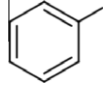
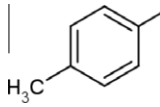
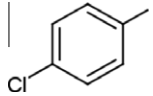
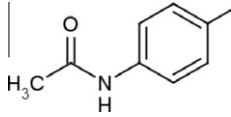
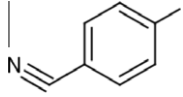
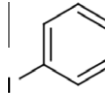
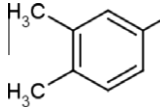
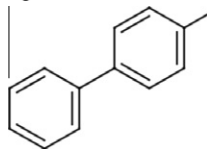
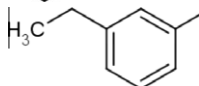
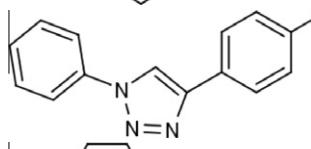
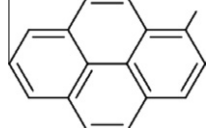
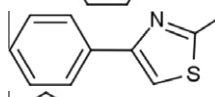
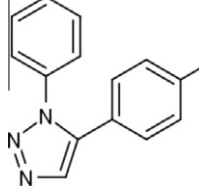
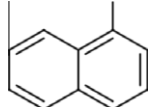
2.2.1. Inhibition of recombinant HDAC enzymes

In a first series, two-step enzyme activity assays with control compounds **24** and **25** were accomplished using HDAH, HDAC1, HDAC6, HDAC7 and HDAC8. All K_d-values were summarized in Table 1. Obtained results confirm SAHA (**25**) as a suitable reference inhibitor for HDAH, HDAC1, HDAC6 and HDAC8. Class IIa HDAC7 was only weakly inhibited by SAHA which is in accordance to Bradner et al.¹⁰ The dianilide reference compound **24** was only a very weak inhibitor of HDAH (55 ± 5.5 μM). In accordance to SAHA, compound **4** showed a significant inhibition of HDAH, HDAC1, HDAC6 and HDAC7. HDAC8 is lesser favored with an K_d-value of



Scheme 1. Synthesis scheme for hydroxamic acid compounds with perfluorinated spacer. Compound **3** served as chemical starting point for the synthesis of all perfluorinated hydroxamic acids.

Table 1
Selectivity profile of perfluorinated hydroxamic acids against HDAH and different HDAC isoforms

ID		HDAH	HDAC1	HDAC6	HDAC7	HDAC8
4		0.54 ± 0.02	29 ± 5.3	11 ± 2.1	11 ± 1.0	17 ± 0.6
5		0.27 ± 0.02	14 ± 1.1	>100	52 ± 38	34 ± 5.3
6		0.21 ± 0.02	12 ± 2.9	23 ± 4.7	19 ± 6.3	35 ± 2.8
7		1.3 ± 0.23	18 ± 2.8	9.2 ± 1.7	13 ± 5.4	36 ± 4.6
8		0.23 ± 0.01	18 ± 1.3	71 ± 35	32 ± 4.1	35 ± 3.8
9		0.39 ± 0.03	14 ± 8.8	4.2 ± 1.0	4.1 ± 0.37	36 ± 5.4
10		0.26 ± 0.02	8.8 ± 1.0	24 ± 13	3.3 ± 0.52	14 ± 1.0
11		3.8 ± 1.1	31 ± 13	49 ± 36	14 ± 0.8	57 ± 17
12		0.19 ± 0.02	16 ± 4.4	1.3 ± 0.22	3.0 ± 0.41	13 ± 1.4
13		7.0 ± 1.0	>100	8.2 ± 2.0	30 ± 6.6	>100
14		0.6 ± 0.2	22 ± 5.8	17 ± 4.3	75 ± 33	47 ± 11
15		2.2 ± 0.2	2.6 ± 0.2	5.4 ± 1.3	1.4 ± 0.17	1.5 ± 0.28
16		4.5 ± 0.5	66 ± 6.5	47 ± 9.2	12 ± 2.2	>100
17		0.37 ± 0.03	29 ± 2.6	32 ± 8.3	20 ± 4.1	19 ± 5.9

(continued on next page)

Table 1 (continued)

ID		HDAH	HDAC1	HDAC6	HDAC7	HDAC8
18		0.45 ± 0.05	30 ± 5.7	15 ± 4.7	14 ± 0.9	60 ± 25
19		0.16 ± 0.02	12 ± 0.3	6.8 ± 1.75	11 ± 0.8	49 ± 12
20		0.86 ± 0.05	49 ± 6.0	9.2 ± 0.9	14 ± 2.9	5.3 ± 0.47
21		9.1 ± 0.8	65 ± 14	>100	38 ± 8.3	60 ± 39
22		0.29 ± 0.04	18 ± 2.3	10 ± 1.9	11 ± 1.4	5.3 ± 0.8
23		0.74 ± 0.06	14 ± 1.2	5.9 ± 0.73	13 ± 2.2	1.4 ± 0.25
24		27 ± 2.7	>100	>100	>100	>100
25		0.30 ± 0.02	0.04 ± 0.01	0.30 ± 0.07	36 ± 16	2.9 ± 0.20

The values correspond to K_d -values (in μM) of the corresponding compound tested against one of the denoted purified recombinant HDAC homologues determined by using fluorogenic enzyme activity assays as described in Section 5.

17 ± 0.6 μM . While **4** inhibited HDAH with almost the same potency than SAHA, HDAC1 was inhibited 725 times and HDAC6 37 times weaker when compared with SAHA. And **4** is 6 times less potent against HDAC8 than SAHA. In contrast, **4** inhibits class IIa HDAC7 with about three times higher potency than SAHA indicating a completely different selectivity profile of both analogs. While introduction of one *p*-methyl group (**5**) caused a slight preference for HDAC1 and HDAH, substitution with a second methyl residue in *meta* position (**10**) led to a significant inhibition of HDAC7 at a K_d -value of 3.3 ± 0.52 μM (Table 1). Compounds with *para*-chlorine (**6**) or *para*-iodine (**9**) substitutions inhibited HDAH and HDAC1 similarly. However, iodine (**9**) induces a noticeable inhibition for HDAC6 (4.2 ± 1.0 μM) and HDAC7 (4.1 ± 0.37 μM) as well. Compound **7** having an acetyl amino group shows a moderate inhibition of all investigated HDAC homologs except for HDAC8. The introduction of a *para*-cyano group (**8**) resulted in a diminished inhibition of class II HDACs. The steric conditions at the outer rim of the active site of the HDAC homologs were further explored using biphenyl capping groups that were substituted in *para*- (**11**), *meta*- (**18**) and *ortho*- (**20**) positions of one phenyl ring by the per-fluorinated linker with terminal hydroxamic acid functional group. It turned out that *para*-substitution in general had an unfavorable impact on the potency of all HDAC homologs except for HDAC7.

meta-Substitution had only a negative impact on inhibition of HDAC8, whereas the relatively bulky *ortho*-substitution caused weaker inhibition of HDAC1 but improved the inhibition of HDAC8. Apart from a slight decreased potency of **19** against HDAC8 the naphthalene derivatives **17** and **19** showed only moderate differences in IC_{50} values to SAHA analog **4**. When proceeding to the enlarged ring system of anthracene, the difference between the substitution in position 1 (**23**) and 2 (**21**) became more obvious. Interestingly, the potency of the potentially bulkier **23** remained almost the same against all HDAC homologs except for HDAC8 when compared with **4**. Though being much bulkier, **23** inhibited HDAC8 10 times stronger than **4**. On the other hand the potentially more elongated compound **21** exhibited pronounced lower potency against all HDAC homologs.

Compounds **13** and **16** containing triazol capping groups showed reduced potency on most HDAC isoforms as compared to compound **4**. Both compounds showed similar decreased potency against the bacterial HDAH and no or very low inhibition of class I HDACs 1 and 8 (Fig. 1). On the other hand compound **13** showed a moderate selectivity for HDAC6 ($K_d = 8.2 \pm 2.0 \mu\text{M}$) whereas compound **16** showed slight selectivity for HDAC7 ($K_d = 12 \pm 2.2 \mu\text{M}$). The thiazole containing compound **15** is a strong but rather unselective inhibitor of all investigated HDAC homologs. In addition, it

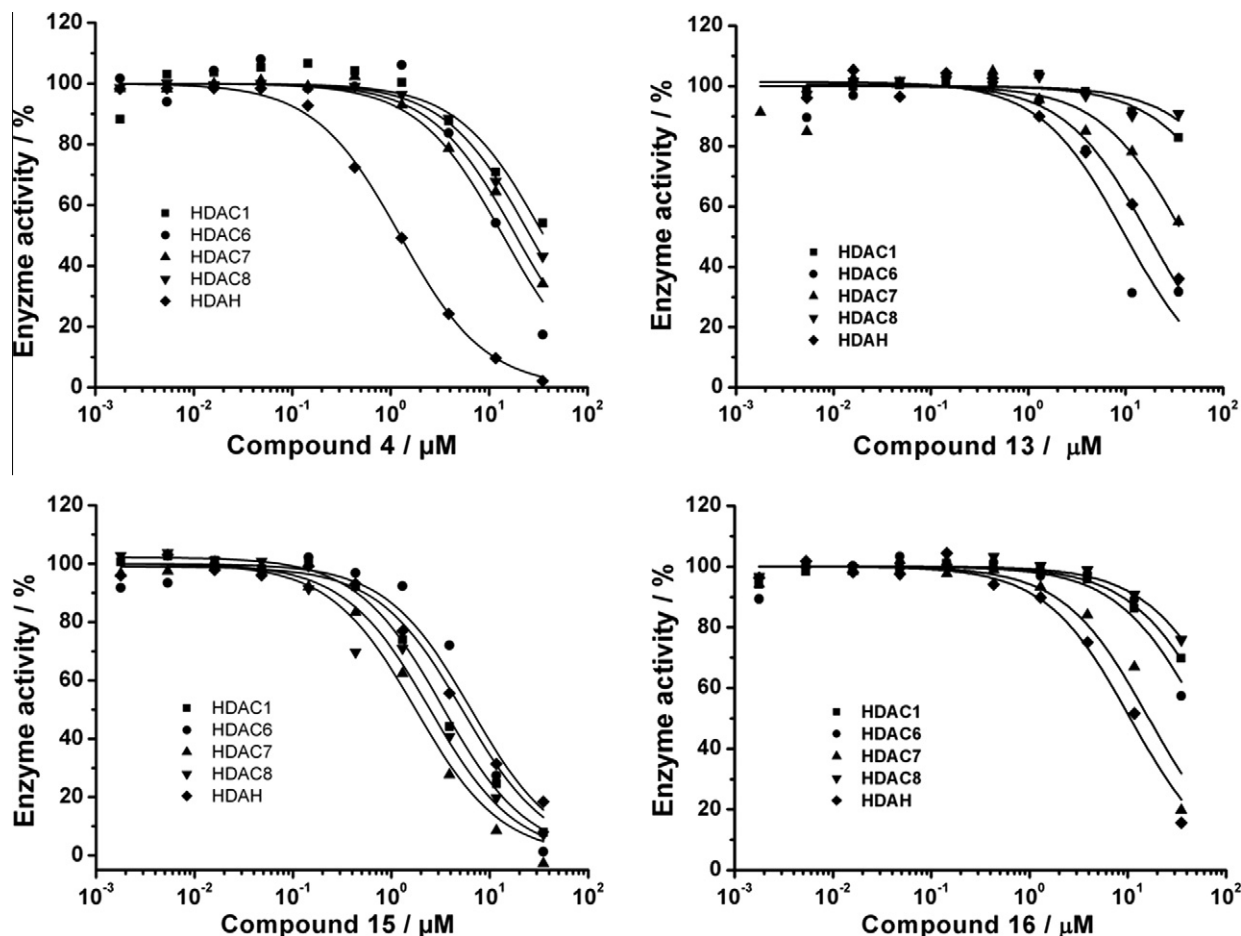


Figure 1. Selectivity profiles of selected perfluorinated SAHA analogs. Dose–response curves were performed using the enzyme-activity assays as described in Section 5. The normalized enzyme activity refers to a reaction mixture in the absence of inhibitor compounds and is plotted versus the concentration of the respective compound.

could be shown, that **4** displaced the fluorescent Atto-hydroxamate ligand from its location of binding within the active site of HDAH in a dose-dependent manner (Fig. 2) confirming the active site to be the local target of interaction for the inhibitor. The binding constant between HDAH and **4** was calculated to be $0.4 \pm 0.1 \mu\text{M}$ according to the method of Riester et al.¹⁴

2.2.2. Inhibition of cellular HDACs

Selected by potency, compounds **4**, **7**, **9**, **10**, **12**, **15**, **19**, **20**, **23** were subjected to a two-step-assay in the presence of diluted cell lysate, instead of purified recombinant human HDACs. The cell lysate was obtained under natural conditions from human K562 cells. The activity of all HDAC isoforms was addressed by two substrates which are known to be processed by either class I HDACs 1,2,3 and HDAC 6 (Boc-L-Lys(acetyl)-MCA) or class IIa HDACs 4,5,7,9 and HDAC 8 (Boc-L-Lys(trifluoroacetyl)-MCA).¹⁵

The resulting IC_{50} values were summarized in Table 2. Only compound **15** showed significant but rather unselective inhibition of the cellular HDACs using both substrates. The corresponding IC_{50} values were $30 \pm 3.2 \mu\text{M}$ for Boc-L-Lys(acetyl)-MCA and $14 \pm 1.7 \mu\text{M}$ for Boc-L-Lys(trifluoroacetyl)-MCA, respectively.

2.3. Molecular docking and simulation study

Blind docking of reference compound SAHA and its perfluorinated derivative **4** into the 3D-structure of a homology model of HDAC1 and X-ray structures of HDAH (1ZZ1) and HDAC8 (1T67) was performed to look for potential binding sites and to obtain a

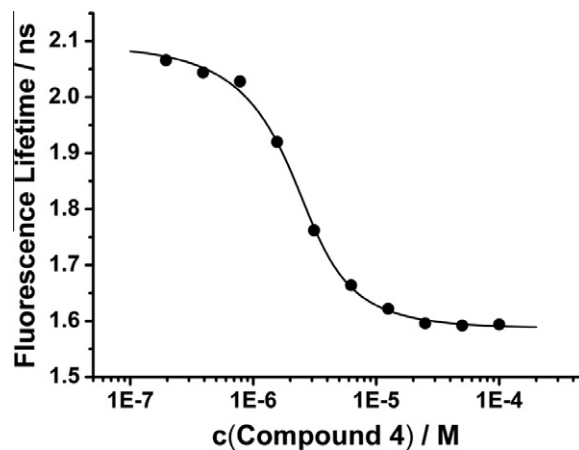


Figure 2. Binding isotherm of compound **4** to HDAH. The binding of compound **4** to $2.5 \mu\text{M}$ HDAH was assessed at 21°C using the dual parameter competition assay under standard assay condition employing 50 nM of Atto-ligand probe and denoted concentrations of compound **4**. The change of fluorescence lifetime of the fluorescent probe upon its displacement from HDAH indicated binding of compound **4**. The straight line represents a data fit to a competitive binding model yielding a binding constant of $0.4 \mu\text{M}$.

suitable starting point for subsequent molecular dynamics (MD) simulations. The ligand structures of more than 100 docking poses were clustered according to RMSD values for each protein–ligand complex. The energetically most favorable clusters of both, SAHA

Table 2
Inhibition of native HDACs from K562 cell lysate

Compounds	Boc-Lys-(acetyl)-MCA	Boc-Lys-(trifluoroacetyl)-MCA
4	>50	49 ± 2.9
7	>50	>50
9	>50	>50
10	>50	>50
12	>50	42 ± 3.4
15	30 ± 3.2	14 ± 1.7
19	>50	45 ± 3.8
20	>50	>50
23	>50	>50

The values correspond to IC_{50} values (in μM) of the corresponding compound tested in the presence of K562 cell lysate using two different fluorogenic substrates (Boc-Lys-(acetyl)-MCA and Boc-Lys-(trifluoroacetyl)-MCA).

and **4**, were always located in the active sites of HDAH and human HDACs 1 and 8 (see Supplementary Figs. S1–S3). For both complexes, HDAH with SAHA and **4**, the corresponding energetically most favorable poses were taken as starting points for energy minimization and cascading MD simulations at increasing temperatures according to the protocol described in Section 5. The potential energies of both complexes showed no skewness over the final 2 ns MD run but rather scattered around a constant value, indicating an equilibrated system (see Supplementary Fig. S4). The structurally aligned protein structures achieved equilibrium after about 500 ps when no significant changes of the root mean square distance (RMSD) could be observed. In contrast, the RMSD values of the small ligands fluctuated much more reflecting the flexibility of the free rotatable phenyl capping group and to a lesser extent the spacer (see Supplementary Fig. S5). The final complex structures with both ligands were matched by minimizing the RMSD between the corresponding proteins. Both ligands were shown to form bidentate complexes with the catalytic Zn^{2+} and to have similar orientations within the active site (Fig. 3).

3. Discussion

SAHA is a rather unselective inhibitor for all class I and class IIb HDACs¹⁰ and an FDA approved cancer drug. Actually, SAHA is also investigated in numerous clinical trials¹⁶ to extend its clinical indication from cutaneous T cell lymphoma to other types of cancer. Based on its chemical structure a new scaffold with perfluorated alkyl chain was created (Scheme 1). The linker region was supposed to change its electronic charge distribution and hydrophobic character, due to the substitution of the 12 hydrogen atoms by highly electronegative fluorine atoms. This became already noticeable during synthesis of the activated perfluorinated spacer intermediate which could not be obtained as anhydride like in the standard synthesis of SAHA¹² but rather as an acid dichloride. However, compound **4** as the closest analog to SAHA showed noticeable inhibition of HDAH and also of all tested recombinant HDACs even though its selectivity profile was clearly distinct from SAHA. While the potency of **4** and SAHA against HDAH was comparable, compound **4** turned out to inhibit human classes I and IIb HDACs 6–360 times weaker whereas **4** was about 3 times more potent against class IIa member HDAC7. This was the first hint that the perfluorated scaffold could contribute to class II selectivity. The negative control **24** lacking the hydroxamate moiety achieved no significant inhibition of any HDAC homolog indicating no obvious unspecific contribution of the newly introduced perfluorinated spacer. Obtained results from **4** and **24** necessitate the presence of the Zn^{2+} chelating hydroxamate group for efficient inhibition of HDACs. The graduated IC_{50} values of the synthesized compounds **5–23** with respect to different HDAC isoform from classes I, IIa

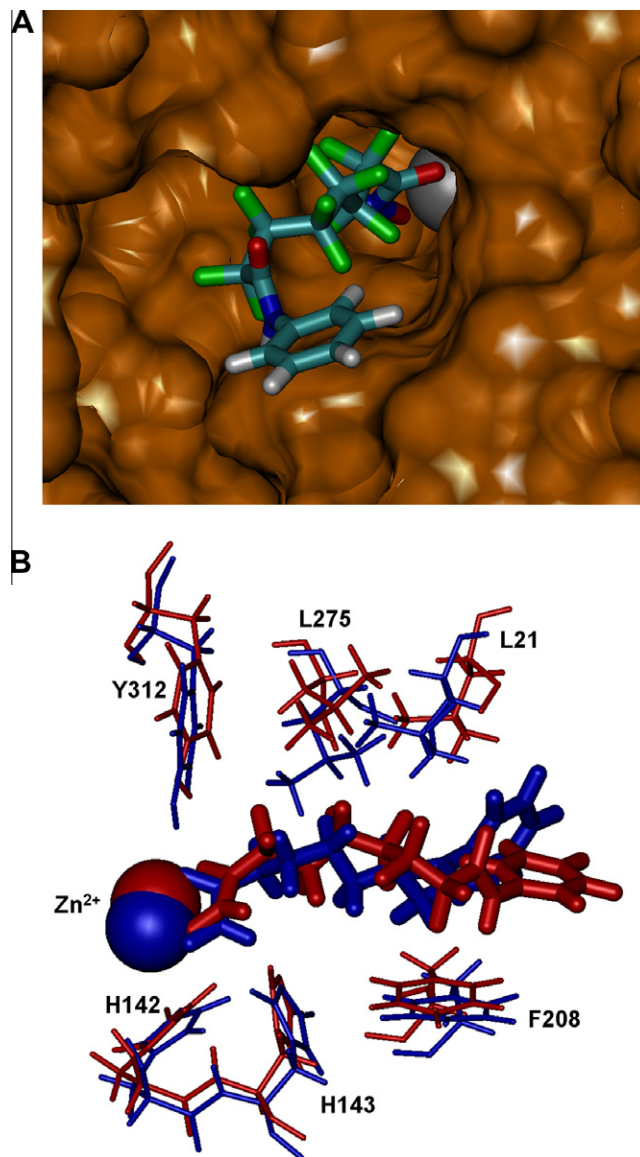


Figure 3. MD-simulations of protein–ligand complexes consisting of HDAH and SAHA or its perfluorinated analog (**4**). The inhibitor molecules were docked into the 3D-structure of HDAH (PDB 1ZZ1 chain C) and subsequently subjected to MD-simulations. The final complex structures were matched by minimizing the root mean square deviation between the proteins. (A) Final pose of MD-simulation: Perfluorinated SAHA formed a bidentate complex with the Zn^{2+} ion (gray bead) at the bottom of the active site of HDAH. (B) Overlay of the active site of HDAH in complex with SAHA (blue) and its perfluorinated analog **4** (red).

and IIb and HDAH proved the potential of SAHA analogs with a perfluorinated substructure (Table 1).

Moreover, compounds differing in their cap groups, developed distinct selectivity profiles with varying potencies. In general, compounds **5–10** and **12** with smaller substituents exhibited similar IC_{50} values for HDAH, and class I HDACs 1 and 8. The iodine and ethyl substituted analogs **9** and **12**, respectively, showed a moderate preference for class II HDACs 6 and 7 confirming the potential to create class II selectivity using the perfluoroalkyl-hydroxamate scaffold. Three of our compounds (**5**, **10** and **12**) directly corresponded to compounds **4**, **12** and **6** in Oger's study¹⁷ of SAHA analogs differing only in the perfluorination of the spacer. Interestingly, the moderate class IIa/IIb preference of our compounds **10** and **12** was not observed for the corresponding unfluorinated counterparts. Moreover, the SAHA analogs with plain alkyl chains exhibited a distinct selectivity for HDAC1 and HDAC6 but not for

HDAC7. This direct comparison between perfluorinated and unfluorinated SAHA analogs suggests that the perfluorinated linker itself contributes to the induction of selectivity for HDAC class II, particularly class IIa.

Inspired by these results and assuming an inhibition binding mode similar to that of SAHA, we tried to generate even stronger differentiating selectivity profiles by synthesizing perfluorinated SAHA analogs with bulkier substitutions at the aromatic ring. Trying biphenyl capping groups (**11**, **18**, **20**) differently attached to the perfluorinated hydroxamate scaffold the *para*-substitution interfered with the activity of all HDACs except for HDAC7 and *ortho*-substitution increased the potency of **20** against HDAC8 to an K_d -value of $5.3 \pm 0.47 \mu\text{M}$. Using differently attached naphthalene capping groups (**17**, **19**) also showed no significant improvement of compound selectivity profiles. The bulkier anthracene capping group attached at position 2 (**21**) caused a drop in potency against HDAH and all human HDACs. When anthracene is attached to the perfluorinated hydroxamate scaffold via position 1 (**23**), the IC_{50} values of HDAH, HDAC1, HDAC6 and HDAC7 become similar to the closest SAHA analog compound **4**. Moreover, **23** was an about 10 times more potent inhibitor of HDAC8 than **4** indicating that the anthracene capping group undergoes additional presumably hydrophobic interaction with the surface of HDAC8. Combining the results of the compounds with biphenyl and anthracene capping groups, more elongated structures are supposed to lead to unfavorable HDAC inhibitors, in general. On the other hand, more bulkier cap group substitutions seemed to favor the inhibition of HDAC8 and in general not to decrease the inhibitory potency against the other HDAC homologs. The introduction of capping groups containing triazol rings leads to compounds **13** and **16** and reduced potency against HDAH and class I HDACs. Both compounds appeared to be moderately selective for class II HDACs. Since **13** showed a moderate preference for HDAC6 whereas **16** was slightly selective for HDAC7, systematic variations of triazol based capping groups may enable to tune the selectivity profile with respect to class IIa or IIb. Compound **15** is the only compound in our series of novel HDAC inhibitors where the phenyl ring of perfluorinated SAHA analogs is replaced by a thiazole heterocycle that is substituted by another phenyl ring. Compound **15** turned out to be an unselective and comparable strong inhibitor of all human HDACs and HDAH even though its potency against HDAC1 and HDAC6 is much lower than that of SAHA. On the other hand **15** was found to be about 25 times more potent against HDAC7 and twice as potent against HDAC8 than SAHA. Consistent with its allosteric inhibitory effect on all recombinant HDACs, **15** was able to inhibit the processing of two different substrates with complementary isoform selectivity by native HDAC multi-enzyme complexes in K562 cellular lysate. The IC_{50} values of, for example **15** or **12** in the lysate of K562 cells were significantly higher compared with those of the biochemical assay using recombinant HDACs. In fact, only **15** was found to be a clear but rather weak inhibitor of human HDACs in the cell lysate. This might be explained by an increased disposition for unspecific binding to the surface of hydrophobic proteins. This hypothesis is backed by our finding that addition of BSA to the enzyme activity assay using purified recombinant HDACs clearly reduced the potency of perfluorinated SAHA analogs *in vitro* (unpublished results).

The inhibition of HDAH and human HDACs by perfluorinated analogs of SAHA has been proven but the exact location of the binding site was not clear *a priori*. In principle, inhibitors could bind to the active site or to other allosteric sites on the surface of an enzyme. The question of the actual binding site was examined by blind docking, molecular dynamics (MD) simulations and experimentally by a competitive binding assay using a fluorescent Atto-hydroxamate ligand probe. Blind docking revealed a definite preference of both, SAHA and its analog **4**, for binding to the active

sites of HDAH, HDAC1 and HDAC8. Subsequent MD simulations demonstrated similar orientations of SAHA and **4** within the active site of HDAH. However, the ligand structures showed pronounced fluctuations indicating the necessity of prolonged MD simulations to improve the understanding of the molecular base of ligand–enzyme interaction. In the competitive binding assay compound **4**, the perfluorinated analog of SAHA, acted as a competitive ligand displacing the fluorescent probe Atto-hydroxamic acid, which has been shown to bind to the Zn^{2+} containing active site of HDAH¹⁴, from its binding site (Fig. 2). This finding confirmed the blind docking and MD simulation results with HDAH and provided strong evidence that **4** and presumably the other perfluorinated analogs of SAHA, as well, bind to the active site of HDAH and probably also of human HDACs. The corresponding binding constant of $0.4 \mu\text{M}$ was in good agreement with the K_d -value ($0.5 \mu\text{M}$, see Table 1) calculated from the IC_{50} -value of the enzyme activity assay.

4. Conclusion

In summary, we proved the potential of compounds with perfluorinated alkyl spacer as HDAC inhibitors. Binding displacement experiments and combined blind docking and MD simulations suggest the perfluorinated analogs of SAHA to bind to the active site of HDAH as well as human HDACs. The replacement of the ordinary alkyl spacer in SAHA and its analogs by perfluorinated alkyl chains created completely different selectivity profiles against different HDAC isoforms. In contrast to the alkyl spacer of SAHA and derivatives, the perfluorinated alkyl spacer seems to contribute to or facilitate the induction of selectivity for class II, particularly class IIa, HDACs even though the overall potency of the perfluorinated SAHA analogs in this study against human HDACs remained still rather moderate. However, when designing novel selective class II inhibitors attention should not exclusively be paid to the capping group and to the distance between capping and zinc binding group but also to the chemistry of the spacer itself, particularly consisting of partially or fully fluorinated linker structures.

5. Experimental section

TLC was performed on TLC aluminium sheets—Silica Gel 60 F254 (Merck). Column chromatography was performed on silica gel 40–63 mesh, (Merck). ¹H NMR-spectra were measured on a Bruker Avance (300.13 MHz) and the ¹⁹F NMR-spectra were measured on a Bruker DRX-400 (376.33 MHz) in CDCl₃ or DMSO-*d*₆ and referenced to TMS. ¹⁹F NMR-spectra were referenced to hexafluorobenzene as external standard. Mass spectra were measured on a Finnigan LCQ^{DECA} (Thermoquest) using APCI (negative mode). Chemicals and solvents were purchased from Sigma–Aldrich, VWR, Alfa Aesar and Fisher Scientific.

5.1. General synthesis for 2,2,3,3,4,4,5,5,6,6,7,7-dodecafluorooctanedioyldichloride

2,2,3,3,4,4,5,5,6,6,7,7-Dodecafluorooctanedioic acid (25.00 g, 64.09 mmol) was poured into a flame dried three necked flask cooled under a nitrogen atmosphere. Thionylchloride (28.0 ml, 45.67 g, 383.9 mmol) was added via a dropping funnel and DMF (8 drops) was added carefully to the colorless suspension. The reaction mixture was refluxed for 4 h. After completion of the reaction remaining thionylchloride was distilled off. The product was obtained as colorless oil by subsequent distillation of the residue under reduced pressure (bp 93–96 °C/100 mbar). Yield: 23.46 g (54.95 mmol); 86%; C₈Cl₂F₁₂O₂; M = 426.97 g/mol; ¹⁹F NMR (CDCl₃): δ (ppm) = –117.6–(–117.8) [m, 4F]; –125.8–(–126.0) [m, 8F].

5.2. General synthesis of benzyl-7-chlorocarbonyl-2,2,3,3,4,4,5,5,6,6,7,7-dodecafluoroheptanoate

5.2.1. The general synthesis followed two different standard procedures, described below

5.2.1.1. Procedure 1. 2,2,3,3,4,4,5,5,6,6,7,7-Dodecafluoro-octanedioyldichloride (23.46 g, 54.95 mmol) was poured into a flame dried three necked flask cooled under a nitrogen atmosphere. The starting material was cooled in an ice bath, before benzyl alcohol (3.40 ml, 3.55 g, 32.83 mmol) was added via a dropping funnel under vigorous stirring over a period of 1 h. The ice bath was removed and the reaction mixture was heated at 100 °C for one additional hour. After cooling to room temperature excessive starting material was collected by distillation under reduced pressure (bp 93–96 °C/100 mbar). High vacuum distillation of the residue provided the product as colorless oil (bp 90–92 °C/0.1 mbar). Yield: 7.70 g (15.44 mmol); 47%

5.2.1.2. Procedure 2. 2,2,3,3,4,4,5,5,6,6,7,7-Dodecafluoro-octanedioyldichloride (18.16 g, 42.53 mmol) was dissolved in 50 ml dioxan and poured into a flame dried three necked flask cooled under a nitrogen atmosphere. The colorless solution was heated in an oil bath at 50 °C. A solution of benzyl alcohol (3.10 ml, 3.24 g, 29.96 mmol) in 25 ml dioxan was added drop wise over a period of 90 min. The reaction mixture was stirred at 100 °C for additional 20 h. After cooling to room temperature the solvent was removed by distillation in vacuo. High vacuum distillation of the residue provided the product as colorless oil (bp 90–92 °C/0.1 mbar).

Yield: 6.83 g (13.70 mmol); 46%; $C_{15}H_7ClF_{12}O_3$; $M = 498.65$ g/mol; 1H NMR ($CDCl_3$): δ (ppm) = 5.27 [s, 2H]; 7.24–7.41 [m, 5H]; ^{19}F NMR ($CDCl_3$): δ (ppm) = –113.9–(–114.1) [m, 2F]; –119.4–(–119.6) [m, 2F]; –122.1–(–122.5) [m, 4F]; –122.6–(–122.9) [m, 2F]; –123.5–(–123.8) [m, 2F].

5.3. Cap group synthesis

5.3.1. Introduction of new cap groups was accomplished by the following standard procedures

5.3.1.1. Standard procedure 1. *5.3.1.1.1. First step.* Benzyl-7-chlorocarbonyl-2,2,3,3,4,4,5,5,6,6,7,7-dodecafluoroheptanoate (0.50 g, 1.00 mmol) was dissolved in 10 ml THF and poured into a flame dried three necked flask cooled under a nitrogen atmosphere. The colorless solution was cooled in an ice bath. Within 30 min a solution of triethylamine (0.17 ml, 0.12 g, 1.19 mmol) and the particular aromatic amine or heteroaromatic amine (1.00 mmol), respectively in the required amount of THF (10–20 ml) was added via a dropping funnel, maintaining the reaction temperature below 5 °C. The reaction mixture was stirred for 2 h, before the ice bath was removed. After additional stirring for 3 h the solvent was evaporated and the intermediate was purified by column chromatography.

5.3.1.1.2. Second step. A solution of the particular benzyl-7-arylcarbonyl-2,2,3,3,4,4,5,5,6,6,7,7-dodecafluoroheptanoate or benzyl-7-heteroarylcarbonyl-2,2,3,3,4,4,5,5,6,6,7,7-dodecafluoroheptanoate, respectively in 10 ml abs THF ($C_{res} = 0.043$ mmol/ml) was treated via syringe with the required amount of 1.0-M hydroxylamine (2.0 equiv) in THF. The reaction mixture was stirred at room temperature for 24 h. After evaporation of the solvent the product was isolated by column chromatography.

5.3.2. Standard procedure 2

Benzyl-7-chlorocarbonyl-2,2,3,3,4,4,5,5,6,6,7,7-dodecafluoroheptanoate (0.50 g, 1.00 mmol) was dissolved in 10 ml THF and poured into a flame dried two necked flask cooled under a nitrogen atmosphere. The colorless solution was cooled in an ice bath.

Within 30 min a solution of triethylamine (0.17 ml, 0.12 g, 1.19 mmol) and the particular aromatic amine or heteroaromatic amine (1.00 mmol), respectively in the required amount of THF (10–20 ml) was added via a dropping funnel, maintaining the reaction temperature below 5 °C. The reaction mixture was stirred for 2 h. After additional stirring for 3 h at room temperature 1.0 M hydroxylamine (2.00 ml, 2.00 mmol) in THF was added via syringe. The reaction mixture was stirred at room temperature until TLC indicated complete consumption of the intermediate. The solvent was evaporated and the product was isolated by column chromatography.

5.3.3. 2,2,3,3,4,4,5,5,6,6,7,7-Dodecafluoro-octanedioic acid hydroxyamide phenyl-amide (4)

Using aniline (0.10 ml; 0.10 g; 1.07 mmol) as starting material the product was obtained as a colorless solid according to standard procedure 2.

Yield: 0.07 g (0.15 mmol); 14% $C_{14}H_8F_{12}N_2O_3$; $M = 480.21$ g/mol; 1H NMR ($DMSO-d_6$): δ (ppm) = 7.28–7.38 (m, 1H); 7.46–7.53 (m, 2H); 7.71–7.81 (m, 2H); 9.97 (s, br, 1H); 11.36 (s, br, 1H); 12.41 (s, br, 1H); ^{19}F NMR ($DMSO-d_6$): δ (ppm) = –117.5–(–117.8) [m, 2F]; –118.1–(–118.5) [m, 2F]; –120.7–(–121.3) [m, 4F]; –121.5–(–121.7) [m, 2F]; –121.8–(–122.0) [m, 2F]; MS (–p APCI): $m/z = 479$ (100%) [M–1][–].

5.3.4. 2,2,3,3,4,4,5,5,6,6,7,7-Dodecafluoro-octanedioic acid hydroxyamide 4-methyl-phenylamide (5)

Using 4-methylaniline (0.11 ml; 0.11 g; 1.03 mmol) as starting material the product was obtained as a yellowish solid according to standard procedure 2.

Yield: 0.09 g (0.18 mmol); 17%; $C_{15}H_{10}F_{12}N_2O_3$; $M = 494.23$ g/mol; 1H NMR ($DMSO-d_6$): δ (ppm) = 2.34 (s, 3H); 7.21–7.29 (m, 2H); 7.52–7.60 (m, 2H); 9.97 (s, br, 1H); 11.19 (s, br, 1H); 12.36 (s, br, 1H); ^{19}F NMR ($DMSO-d_6$): δ (ppm) = –118.1–(–118.3) [m, 2F]; –119.4–(–119.7) [m, 2F]; –121.5–(–121.9) [m, 4F]; –122.2–(–122.7) [m, 4F]; MS (–p APCI): $m/z = 493$ (100%) [M–1][–].

5.3.5. 2,2,3,3,4,4,5,5,6,6,7,7-Dodecafluoro-octanedioic acid (4-chlorophenyl)amide hydroxyamide (6)

Using 4-chloroaniline (0.13 g; 1.02 mmol) as starting material the product was obtained as a colorless solid according to standard procedure 2.

Yield: 0.07 g (0.14 mmol); 14%; $C_{14}H_7ClF_{12}N_2O_3$; $M = 514.65$ g/mol; 1H NMR ($DMSO-d_6$): δ (ppm) = 7.48–7.53 (m, 2H); 7.69–7.78 (m, 2H); 9.93 (s, br, 1H); 11.41 (s, br, 1H); 12.37 (s, br, 1H); ^{19}F NMR ($DMSO-d_6$): δ (ppm) = –119.5–(–119.7) [m, 2F]; –119.8–(–120.2) [m, 2F]; –121.7–(–122.0) [m, 4F]; –122.3–(–123.1) [m, 4F]; MS (–p APCI): $m/z = 515$ (33%) [M–1][–]; 513 (100%) [M–1][–].

5.3.6. 2,2,3,3,4,4,5,5,6,6,7,7-Dodecafluoro-octanedioic acid (4-acetylaminophenyl)-amide hydroxyamide (7)

Using 4-acetylaminoaniline (0.15 g; 1.00 mmol) as starting material the product was obtained as a yellowish solid according to standard procedure 2.

Yield: 0.07 g (0.11 mmol); 11%; $C_{16}H_{11}F_{12}N_3O_4$; $M = 537.26$ g/mol; 1H NMR ($DMSO-d_6$): δ (ppm) = 2.18 (s, 3H); 7.60–7.82 (m, 4H); 10.03 (s, br, 1H); 10.13 (s, 1H); 11.27 (s, br, 1H); 12.44 (s, br, 1H); ^{19}F NMR ($DMSO-d_6$): δ (ppm) = –118.7–(–119.1) [m, 2F]; –119.5–(–119.9) [m, 2F]; 122.2–(–123.1) [m, 8F]; MS (–p APCI): $m/z = 536$ (100%) [M–1][–].

5.3.7. 2,2,3,3,4,4,5,5,6,6,7,7-Dodecafluoro-octanedioic acid (4-cyanophenyl)amide hydroxyamide (8)

Using 4-aminobenzonitrile (0.12 g; 1.02 mmol) as starting material the intermediate Benzyl 7-(4-cyanophenylcarbonyl)-

2,2,3,3,4,4,5,5,6,6,7,7-dodecafluoroheptanoate was obtained as a colorless solid according to standard procedure 1 step 1.

Yield: 0.15 g (0.26 mmol); 26%; $C_{22}H_{12}F_{12}N_2O_3$; $M = 580.07$ g/mol; 1H NMR (DMSO- d_6): δ (ppm) = 5.58 (s, 2H); 7.45–7.55 (m, 5H); 7.95–8.03 (m, 4H); 11.72 (s, br, 1H); ^{19}F NMR (DMSO- d_6): δ (ppm) = –118.1(–118.4) [m, 4F]; –121.3(–121.7) [m, 4F]; –122.0(–122.2) [m, 2F]; 122.4(–122.7) [m, 2F]; MS (–p APCI): $m/z = 579$ (100%) [M–1] $^-$.

Using benzyl-7-(4-cyanophenylcarbamoyl)-2,2,3,3,4,4,5,5,6,6,7,7-dodecafluoroheptanoate (0.13 g; 0.22 mmol) as starting material the product was obtained as a colorless solid according to standard procedure 1 step 2.

Yield: 0.04 g (0.08 mmol); 36%; $C_{15}H_7F_{12}N_3O_3$; $M = 505.22$ g/mol; 1H NMR (DMSO- d_6): δ (ppm) = 7.96–8.01 (m, 4H); 10.00 (s, br, 1H); 11.73 (s, br, 1H); 12.41 (s, br, 1H); ^{19}F NMR (DMSO- d_6): δ (ppm) = –118.5(–118.9) [m, 2F]; –119.2(–119.6) [m, 2F]; –121.5(–122.4) [m, 8F]; MS (–p APCI): $m/z = 504$ (100%) [M–1] $^-$.

5.3.8. 2,2,3,3,4,4,5,5,6,6,7,7-Dodecafluoroctanedioic acid hydroxyamide (4-iodo-phenyl)amide (9)

Using 4-iodoaniline (0.22 g; 1.00 mmol) as starting material the product was obtained as a colorless solid according to standard procedure 2.

Yield: 0.04 g (0.08 mmol); 8%; $C_{14}H_7F_{12}IN_2O_3$; $M = 606.10$ g/mol; 1H NMR (DMSO- d_6): δ (ppm) = 7.52–7.71 (m, 2H); 7.81–7.89 (m, 2H); 10.01 (s, br, 1H); 11.41 (s, br, 1H); 12.43 (s, br, 1H); ^{19}F NMR (DMSO- d_6): δ (ppm) = –118.5(–118.8) [m, 2F]; –119.3(–119.7) [m, 2F]; –121.4(–121.9) [m, 4F]; –122.0(–122.5) [m, 4F]; MS (–p APCI): $m/z = 605$ (100%) [M–1] $^-$.

5.3.9. 2,2,3,3,4,4,5,5,6,6,7,7-Dodecafluoroctanedioic acid (3,4-dimethylphenyl)-amide hydroxyamide (10)

Using 3,4-dimethylaniline (0.17 ml; 0.12 g; 0.99 mmol) as starting material the product was obtained as a colorless solid according to standard procedure 2.

Yield: 0.04 g (0.08 mmol); 8%; $C_{16}H_{12}F_{12}N_2O_3$; $M = 508.26$ g/mol; 1H NMR (DMSO- d_6): δ (ppm) = 2.19–2.28 (m, 6H); 7.11–7.20 (m, 1H); 7.33–7.40 (m, 1H); 7.42–7.48 (m, 1H); 9.92 (s, br, 1H); 11.11 (s, br, 1H); 12.35 (s, br, 1H); ^{19}F NMR (DMSO- d_6): δ (ppm) = –118.2(–118.5) [m, 2F]; –119.1(–119.5) [m, 2F]; –121.5(–121.8) [m, 4F]; –122.0(–122.5) [m, 4F]; MS (–p APCI): $m/z = 507$ (100%) [M–1] $^-$.

5.3.10. 2,2,3,3,4,4,5,5,6,6,7,7-Dodecafluoroctanedioic acid biphenyl-4-ylamide hydroxyamide (11)

Using biphenyl-4-ylamine (0.17 g; 1.00 mmol) as starting material the product was obtained as a colorless solid according to standard procedure 2.

Yield: 0.08 g (0.14 mmol); 14%; $C_{20}H_{12}F_{12}N_2O_3$; $M = 556.30$ g/mol; 1H NMR (DMSO- d_6): δ (ppm) = 7.31–7.39 (m, 1H); 7.39–7.53 (m, 2H); 7.67–7.82 (m, 6H); 9.97 (s, br, 1H); 11.36 (s, br, 1H); 12.36 (s, br, 1H); ^{19}F NMR (DMSO- d_6): δ (ppm) = 116.9(–117.1) [m, 2F]; –117.7(–118.0); [m, 2F]; –120.3(–120.6) [m, 4F]; –121.0(–121.2) [m, 2F]; –121.3(–121.5) [m, 2F]; MS (–p APCI): $m/z = 555$ (100%) [M–1] $^-$.

5.3.11. 2,2,3,3,4,4,5,5,6,6,7,7-Dodecafluoroctanedioic acid (3-ethylphenyl)amide hydroxyamide (12)

Using 3-ethylaniline (0.12 ml; 0.12 g; 1.00 mmol) as starting material the product was obtained as a colorless solid according to standard procedure 2.

Yield: 0.13 g (0.26 mmol); 26%; $C_{16}H_{12}F_{12}N_2O_3$; $M = 508.26$ g/mol; 1H NMR (DMSO- d_6): δ (ppm) = 1.17–1.21 (t, 3H, $^3J = 7.0$ Hz); 2.57–2.68 (q, 2H, $^3J = 7.0$ Hz); 7.07–7.13 (m, 1H); 7.29–7.37 (m, 1H); 7.47–7.55 (m, 1H); 9.95 (s, br, 1H); 11.19 (s, br, 1H); 12.35 (s, br, 1H); ^{19}F NMR (DMSO- d_6): δ

(ppm) = –116.9(–117.2) [m, 2F]; –117.6(–117.9) [m, 2F]; –120.3(–120.6) [m, 4F]; –121.0(–121.3) [m, 2F]; –121.3(–121.6) [m, 2F]; MS (–p APCI): $m/z = 507$ (100%) [M–1] $^-$.

5.3.12. 2,2,3,3,4,4,5,5,6,6,7,7-Dodecafluoroctanedioic acid hydroxyamide (4-[1-phenyl-1H-(1,2,3)triazol-4-yl]phenyl)amide (13)

Using 4-(4-aminophenyl)-1-phenyl-1H-[1,2,3]-triazole (0.24 g; 1.02 mmol) as starting material the product was obtained as a colorless solid according to standard procedure 2.

Yield: 0.23 g (0.37 mmol); 36%; $C_{22}H_{13}F_{12}N_5O_3$; $M = 623.35$ g/mol; 1H NMR (DMSO- d_6): δ (ppm) = 7.39–7.56 (m, 2H); 7.59–7.71 (m, 2H); 7.78–7.88 (m, 2H); 7.92–8.02 (m, 5H); 9.32 (s, 1H); 11.38 (s, br, 1H); ^{19}F NMR (DMSO- d_6): δ (ppm) = –113.9(–114.3) [m, 2F]; –117.2(–117.6) [m, 2F]; –120.5(–121.5) [m, 8F]; MS (–p APCI): $m/z = 622$ (4%) [M–1] $^-$; 607 (100%) [M–15] $^-$; 563 (100%) [M–59] $^-$.

5.3.12.1. 4-(4-Aminophenyl)-1-phenyl-1H-[1,2,3]-triazole in Section 5.3.12. was prepared by this way.

A 100 mL 2 necked flask was charged with a mixture of 25 mL *t*-butanol and 25 mL water. Then were added 2.40 g (20.00 mmol) phenylazide and 2.36 g (20.00 mmol; 1 equiv) 4-aminophenylethyne. Afterward were given 2 mL of a 1 M sodium ascorbate solution (2.00 mmol; 0.1 equiv) and 50 mg of copper-II-sulfate pentahydrate (0.20 mmol; 0.01 equiv). The dark green suspension was then heated at 60 °C for 17 h. 50 mL of water were added to the reaction mixture after cooling down to room temperature. The mixture was then filtered and washed with water, giving a beige yellow solid, 3.50 g (14.75 mmol); 74%; $C_{14}H_{13}N_4$; $M = 237.28$ g/mol; 1H NMR (DMSO): δ (ppm) = 5.42 (s, br, 2H); 6.76 (d, 2H); 7.41 (m, 1H); 7.52 (m, 4H); 7.95 (d, 2H); 9.05 (s, 1H); ^{13}C NMR (DMSO): δ (ppm) = 113.94; 117.11; 117.73; 119.74; 126.40; 128.35; 129.83; 136.78; 148.33; 148.95; R_f (diethylether): 0.54.

5.3.13. 2,2,3,3,4,4,5,5,6,6,7,7-Dodecafluoroctanedioic acid hydroxyamide pyren-1-ylamide (14)

Using 1-aminopyren (0.22 g; 1.01 mmol) as starting material the product was obtained as a brownish solid according to standard procedure 2.

Yield: 0.14 g (0.23 mmol); 23%; $C_{24}H_{12}F_{12}N_2O_3$; $M = 604.34$ g/mol; 1H NMR (DMSO- d_6): δ (ppm) = 8.03–8.44 (m, 9H); 9.99 (s, br, 1H); 11.94 (s, br, 1H); 12.43 (s, br, 1H); ^{19}F NMR (DMSO- d_6): δ (ppm) = –117.2(–117.5) [m, 2F]; –118.0(–118.3) [m, 2F]; –120.5(–121.1) [m, 4F]; –121.3(–121.6) [m, 2F]; –121.8(–122.1) [m, 2F]; MS (–p APCI): $m/z = 603$ (100%) [M–1] $^-$.

5.3.14. 2,2,3,3,4,4,5,5,6,6,7,7-Dodecafluoroctanedioic acid hydroxyamide (4-phenylthiazol-2-yl)amide (15)

Using 2-amino-4-phenylthiazole (0.18 g; 1.02 mmol) as starting material the product was obtained as a brownish solid according to standard procedure 2.

Yield: 0.07 g (0.12 mmol); 12%; $C_{17}H_9F_{12}N_3O_3S$; $M = 563.32$ g/mol; 1H NMR (DMSO- d_6): δ (ppm) = 7.37–7.55 (m, 4H); 7.72 (s, 1H); 7.85–7.92 (m, 1H); 9.94 (s, br, 1H); 12.33 (s, br, 1H); 14.45 (s, br, 1H); ^{19}F NMR (DMSO- d_6): δ (ppm) = –116.3(–116.8) [m, 2F]; –118.2(–118.5) [m, 2F]; –120.7(–121.3) [m, 4F]; –121.3(–121.6) [m, 2F]; –121.8(–122.1) [m, 2F]; MS (–p APCI): $m/z = 562$ (100%) [M–1] $^-$.

5.3.15. 2,2,3,3,4,4,5,5,6,6,7,7-Dodecafluoroctanedioic acid hydroxyamide [4-(1-phenyl-1H-[1,2,3]triazol-5-yl)phenyl]amide (16)

Using 5-(4-aminophenyl)-1-phenyl-1H-[1,2,3]-triazole (0.24 g; 1.02 mmol) as starting material the product was obtained as a brownish solid according to standard procedure 2.

Yield: 0.18 g (0.29 mmol); 28%; $C_{22}H_{13}F_{12}N_5O_3$; $M = 623.35$ g/mol; 1H NMR (DMSO- d_6): δ (ppm) = 7.32–7.38 (m, 2H); 7.41–7.49 (m, 2H); 7.54–7.61 (m, 3H); 7.68–7.75 (m, 2H); 8.17 (s, 1H); 9.93 (s, br, 1H); 11.38 (s, br, 1H); 12.38 (s, br, 1H); ^{19}F NMR (DMSO- d_6): δ (ppm) = –114.6–(–114.9) [m, 2F]; –117.7–(–118.0) [m, 2F]; –120.8–121.9 [m, 8F]; MS (–p APCI): $m/z = 622$ (9%) [M–1] $^-$; 607 (72%) [M–15] $^-$; 563 (100%) [M–59] $^-$.

5.3.15.1. The used 5-(4-aminophenyl)-1-phenyl-1H-[1,2,3]-triazole in Section 5.3.15 was prepared according to the following procedure.

A 100 mL 2 necked flask was charged with 50 mL of toluene and 2.36 g (20.00 mmol; 1 equiv) 4-aminophenylethyne. 2.40 g (20.00 mmol) phenylazide were then added and the black solution was heated to reflux for 43 h. The toluene was removed at reduced pressure and the residue was resolved in 2 N hydrochloric acid. Insoluble material was separated and the liquid phase was washed three times with ethylacetate afterward. The aqueous phase was then heated with some charcoal, filtrated and neutralized with concd sodium hydroxide solution. The black material which deposited from the solution was filtrated, dried and crystallized from a mixture of water/ethanol. Brown crystals were then separated and dried.

Yield: 1.2 g (14.75 mmol); 25%; $C_{14}H_{13}N_4$; $M = 237.28$ g/mol; 1H NMR (DMSO): δ (ppm) = 5.39 (s, br, 2H); 6.56 (d, 2H); 6.85 (m, 2H); 7.41 (m, 2H); 7.56 (m, 2H); 7.95 (s, 1H); ^{13}C NMR (DMSO): δ (ppm) = 112.44; 113.59; 127.17; 128.58; 128.75; 129.42; 130.52; 131.63; 138.42; 149.66; R_f (diethylether): 0.58; MS (+p APCI): $m/z = 237$ (100%) [MH $^+$].

5.3.16. 2,2,3,3,4,4,5,5,6,6,7,7-Dodecafluorooctanedioic acid hydroxyamide naph-thalen-1-ylamide (17)

Using naphthalen-1-ylamine (0.14 g; 0.98 mmol) as starting material the product was obtained as a colorless solid according to standard procedure 2.

Yield: 0.06 g (0.11 mmol); 11%; $C_{18}H_{10}F_{12}N_2O_3$; $M = 530.26$ g/mol; 1H NMR (DMSO- d_6): δ (ppm) = 7.56–7.59 (m, 1H); 7.64–7.73 (m, 3H); 7.83–7.91 (m, 1H); 8.04–8.14 (m, 2H); 10.02 (s, br, 1H); 10.62 (s, br, 1H); 12.44 (s, br, 1H); ^{19}F NMR (DMSO- d_6): δ (ppm) = –117.3–(–117.5) [m, 2F]; –118.1–(–118.4) [m, 2F]; –121.4–(–122.3) [m, 4F]; –122.6–(–123.1) [m, 2F]; –123.3–(–123.8) [m, 2F]; MS (–p APCI): $m/z = 529$ (100%) [M–1] $^-$.

5.3.17. 2,2,3,3,4,4,5,5,6,6,7,7-Dodecafluorooctanedioic acid biphenyl-3-ylamide hydroxyamide (18)

Using biphenyl-3-ylamine (0.17 g; 1.00 mmol) as starting material the product was obtained as a beige colored solid according to standard procedure 2.

Yield: 0.08 g (0.14 mmol); 14%; $C_{20}H_{12}F_{12}N_2O_3$; $M = 556.30$ g/mol; 1H NMR (DMSO- d_6): δ (ppm) = 7.39–7.43 (m, 1H); 7.45–7.58 (m, 4H); 7.63–7.73 (m, 3H); 7.94–7.98 (m, 1H); 9.94 (s, br, 1H); 11.35 (s, br, 1H); 12.37 (s, br, 1H); ^{19}F NMR (DMSO- d_6): δ (ppm) = –116.9–(–117.2) [m, 2F]; –117.6–(–117.9) [m, 2F]; –120.0–(–120.4) [m, 4F]; –120.8–(–121.1) [m, 2F]; 121.2–(–121.5) [m, 2F]; MS (–p ESI): $m/z = 555$ (100%) [M–1] $^-$.

5.3.18. 2,2,3,3,4,4,5,5,6,6,7,7-Dodecafluorooctanedioic acid hydroxyamide naph-thalen-2-ylamide (19)

Using naphthalen-2-ylamine (0.14 g; 0.98 mmol) as starting material the product was obtained as a beige colored solid according to standard procedure 2.

Yield: 0.08 g (0.15 mmol); 15%; $C_{18}H_{10}F_{12}N_2O_3$; $M = 530.26$ g/mol; 1H NMR (DMSO- d_6): δ (ppm) = 7.55–7.64 (m, 2H); 7.87–8.04 (m, 1H); 7.91–8.05 (m, 3H); 8.37–8.40 (m, 1H); 10.02 (s, br, 1H); 11.53 (s, br, 1H); 12.42 (s, br, 1H); ^{19}F NMR (DMSO- d_6): δ (ppm) = –116.8–(–117.2) [m, 2F]; –117.6–(–118.0) [m, 2F];

–120.2–(–120.7) [m, 4F]; 121.0–(–121.3) [m, 2F]; –121.4–(–121.7) [m, 2F]; MS (–p ESI): $m/z = 529$ (100%) [M–1] $^-$.

5.3.19. 2,2,3,3,4,4,5,5,6,6,7,7-Dodecafluorooctanedioic acid biphenyl-2-ylamide hydroxyamide (20)

Using biphenyl-2-ylamine (0.17 g; 1.00 mmol) as starting material the product was obtained as a colorless solid according to standard procedure 2.

Yield: 0.07 g (0.13 mmol); 13%; $C_{20}H_{12}F_{12}N_2O_3$; $M = 556.30$ g/mol; 1H NMR (DMSO- d_6): δ (ppm) = 7.31–7.53 (m, 9H); 9.93 (s, br, 1H); 11.05 (s, br, 1H); 12.35 (s, br, 1H); ^{19}F NMR (DMSO- d_6): δ (ppm) = –117.5–(–117.8) [m, 2F]; –118.2–(–118.5) [m, 2F]; –120.8–(–121.3) [m, 4F]; –121.6–(–121.9) [m, 2F]; –121.9–(–122.2) [m, 2F]; MS (–p ESI): $m/z = 555$ (100%) [M–1] $^-$.

5.3.20. 2,2,3,3,4,4,5,5,6,6,7,7-Dodecafluorooctanedioic acid anthracen-2-ylamide hydroxyamide (21)

Using anthracen-2-ylamine (0.20 g; 1.03 mmol) as starting material the product was obtained as a brownish solid according to standard procedure 2.

Yield: 0.08 g (0.14 mmol); 14%; $C_{22}H_{12}F_{12}N_2O_3$; $M = 580.32$ g/mol; 1H NMR (DMSO- d_6): δ (ppm) = 7.48–7.57 (m, 2H); 7.71–7.77 (m, 1H); 8.05–8.28 (m, 3H); 8.48–8.62 (m, 3H); 9.94 (s, br, 1H); 11.51 (s, br, 1H); 12.38 (s, br, 1H); ^{19}F NMR (DMSO- d_6): δ (ppm) = –117.3–(–117.6) [m, 2F]; –118.1–(–118.4) [m, 2F]; –120.8–(–121.3) [m, 4F]; –121.5–(–121.7) [m, 2F]; –121.8–(–122.1) [m, 2F]; MS (–p ESI): $m/z = 579$ (100%) [M–1] $^-$.

5.3.21. 2,2,3,3,4,4,5,5,6,6,7,7-Dodecafluorooctanedioic acid hydroxyamide phenan-thren-9-ylamide (22)

Using phenanthren-9-ylamine (0.20 g; 1.03 mmol) as starting material the product was obtained as a yellowish solid according to standard procedure 2.

Yield: 0.03 g (0.05 mmol); 5%; $C_{22}H_{12}F_{12}N_2O_3$; $M = 580.32$ g/mol; 1H NMR (DMSO- d_6): δ (ppm) = 7.69–7.98 (m, 6H); 8.04–8.11 (m, 1H); 8.89–8.99 (m, 2H); 9.97 (s, br, 1H); 11.63 (s, br, 1H); 12.46 (s, br, 1H); ^{19}F NMR (DMSO- d_6): δ (ppm) = –117.3–(–117.6) [m, 2F]; –118.3–(–118.6) [m, 2F]; –120.7–(–121.2) [m, 4F]; –121.3–(–121.6) [m, 2F]; –121.8–(–122.1) [m, 2F]; MS (–p ESI): $m/z = 579$ (100%) [M–1] $^-$.

5.3.22. 2,2,3,3,4,4,5,5,6,6,7,7-Dodecafluorooctanedioic acid anthracen-1-ylamide hydroxyamide (23)

Using anthracen-1-ylamine (0.20 g; 1.03 mmol) as starting material the product was obtained as a brownish solid according to standard procedure 2.

Yield: 0.10 g (0.17 mmol); 13%; $C_{22}H_{12}F_{12}N_2O_3$; $M = 580.32$ g/mol; 1H NMR (DMSO- d_6): δ (ppm) = 7.55–7.80 (m, 4H); 8.10–8.23 (m, 3H); 8.49 (s, 1H); 8.78 (s, 1H); 10.03 (s, br, 1H); 11.75 (s, br, 1H); 12.48 (s, br, 1H); ^{19}F NMR (DMSO- d_6): δ (ppm) = –117.3–(–117.6) [m, 2F]; –118.3–(–118.5) [m, 2F]; 120.7–(–121.1) [m, 4F]; –121.6–(–121.8) [m, 2F]; –121.9–(–122.2) [m, 2F]; MS (–p ESI): $m/z = 579$ (100%) [M–1] $^-$.

5.4. Molecular simulation

A homology model of HDAC1 was generated on the basis of the recently solved structure of HDAC2¹⁸ using SWISS-MODEL.¹⁹ Homology modeling was rather straightforward, because both sequences share 93.5% identity in a 367 aminoacid overlap. Docking studies of SAHA and the representative compound **4** to the homology model of HDAC1 and the X-ray structures of HDAH (PDB 1ZZ1) and HDAC8 (PDB 1T67) were performed using SwissDock²⁰ in the accurate mode and allowing the side chains to be flexible within 5 Å of any atom of the corresponding ligand in its reference binding mode. For further refinement of the complex structures MD-simu-

lations were performed using Gromacs V. 4.0.7.²¹ with an implemented AMBER-99 forcefield.²² The Particle Mesh Ewald method was used for the treatments of long-range electrostatic interactions. Starting with the docking structures the enzyme–drug complexes were subjected to two steps of energy minimization in vacuo using steepest descent and conjugate gradient method to remove bad van der Waals contacts. Then the protein was solvated in a box of 594 nm³ volume filled with Tip4 water molecules²³ and Na⁺ and Cl[−] ions corresponding to a final concentration of 250 mM NaCl. After another energy minimization of the solvated complex position-restrained dynamics simulations were run to soak the water and the inhibitor into the inhibitor–enzyme complex (200 ps at 100 K, 60 ps at 200 K and 200 ps at 300 K). Finally, a productive MD-simulation was run over 2 ns at 300 K. The data were analyzed using VMD 1.8.7.²⁴

5.5. Fluorogenic two step enzyme activity assay

According to the two-step-assay established by Wegener et al.²⁵ the protein assay was conducted in a total volume of 100 μ l. In short, a fluorogenic substrate attached to a ϵ -amino-acetylated lysine residue becomes deacetylated due to incubation with a corresponding HDAC or HDAH. Subsequently, trypsin digestion cleaves the c-terminal ending of the lysine residue, releasing a fluorescent 7-amino-4-methylcoumarin (ex: 390 nm, em: 460 nm) group. HDAH was prepared according to Hildmann et al.¹¹, and human recombinant HDACs were purchased from BPS BioSciences. Boc-Lys(acetyl)-MCA was a suitable substrate for HDAH [final concentration $c_f = 15 \mu\text{g}/100 \mu\text{l}$], HDAC1 [$c_f = 0025 \mu\text{g}/100 \mu\text{l}$] and HDAC6 [$c_f = 0045 \mu\text{g}/100 \mu\text{l}$]. HDAC7 [$c_f = 0002 \mu\text{g}/100 \mu\text{l}$] and HDAC8 [$c_f = 0011 \mu\text{g}/100 \mu\text{l}$] favored the trifluoroacetylated substitute Boc-Lys(trifluoroacetyl)-MCA. Substrates were applied at final concentrations of 20 μM in all enzyme assays. K_i -values were calculated from IC_{50} -values according to Cheng and Prusoff.²⁶ The K_m -values of HDAH was 14 μM ¹⁵ and the K_m -values of HDAC1, 6, 7, 8 were determined to be 78 μM , 99 μM , 61 μM and 30 μM , respectively.

5.6. Dual parameter competition assay

The dual parameter competition assay introduced recently by Riester et al.¹⁴ was used to measure binding of inhibitors to HDAH at 21 °C. The assay principle exploits the concurrent change of fluorescence anisotropy and FLT upon the reversible binding of the fluorescent Atto700-hydroxamate ligand to the enzyme. The binding of an inhibitor is indicated by the reversal of the fluorescence properties caused by an effective displacement of the ligand probe. Final concentrations of 50 nM Atto-hydroxamate ligand and 2.5 μM HDAH were used.

5.7. Cell culture

K562 cancer cell line was established as a confluent cell culture in RPMI 16040 medium supplemented with 2% L-glutamine, 50 $\mu\text{g}/\text{ml}$ gentamycin and 10% FCS.

5.8. Cell lysis

Prior to lysis the K562 cells underwent centrifugation (2000 rpm) for 5 min. Then the cells were collected and washed

with PBS solution (pH 6.3). Finally, lysis buffer (50 mM Tris–HCl pH 8.5; 1 M NaCl; 1 mM MgCl₂; 1 w/v Triton-X-100) was added up to 5 times of the corresponding pellet volume. The solution was incubated at 37 °C for 2 h.

Acknowledgements

This work was supported by a Grant of the Bundesministerium für Wirtschaft und Technologie of the Federal Republic of Germany. The excellent encouragement of Dr. Ute Jochem is gratefully acknowledged.

Supplementary data

Supplementary data associated with this article can be found, in the online version, at [doi:10.1016/j.bmc.2011.11.041](https://doi.org/10.1016/j.bmc.2011.11.041).

References and notes

- Rice, J. C.; Allis, C. D. *Curr. Opin. Cell Biol.* **2001**, *13*, 263.
- de Ruijter, A. J.; van Gennip, A. H.; Caron, H. N.; Kemp, S.; van Kuilenburg, A. B. *Biochem. J.* **2003**, *370*, 737.
- Gregoret, I. V.; Lee, Y. M.; Goodson, H. V. *J. Mol. Biol.* **2004**, *338*, 17.
- Verdin, E.; Dequiedt, F.; Kasler, H. G. *Trends Genet.* **2003**, *19*, 286.
- Aldana-Masangkay, G. I.; Sakamoto, K. M. *J. Biomed. Biotechnol.* **2011**, *2011*, 875824.
- Witt, O.; Deubzer, H. E.; Milde, T.; Oehme, I. *Cancer Lett.* **2009**, *277*, 8.
- Finnin, M. S.; Donigian, J. R.; Cohen, A.; Richon, V. M.; Rifkind, R. A.; Marks, P. A.; Breslow, R.; Pavletich, N. P. *Nature* **1999**, *401*, 188.
- Paris, M.; Porcelloni, M.; Binaschi, M.; Fattori, D. *J. Med. Chem.* **2008**, *51*, 1505.
- Wu, R.; Lu, Z.; Cao, Z.; Zhang, Y. *J. Am. Chem. Soc.* **2011**, *133*, 6110.
- Bradner, J. E.; West, N.; Grachan, M. L.; Greenberg, E. F.; Haggarty, S. J.; Warnow, T.; Mazitschek, R. *Nat. Chem. Biol.* **2010**, *6*, 238.
- Hildmann, C.; Ninkovic, M.; Dietrich, R.; Wegener, D.; Riester, D.; Zimmermann, T.; Birch, O. M.; Bernegger, C.; Loidl, P.; Schwienhorst, A. *J. Bacteriol.* **2004**, *186*, 2328.
- Mai, A.; Esposito, M.; Bordella, G.; Massa, S. *Org. Prep. Proced. Int.* **2001**, *33*, 391.
- Riester, D.; Wegener, D.; Hildmann, C.; Schwienhorst, A. *Biochem. Biophys. Res. Commun.* **2004**, *324*, 1116.
- Riester, D.; Hildmann, C.; Haus, P.; Galetovic, A.; Schober, A.; Schwienhorst, A.; Meyer-Almes, F. *J. Bioorg. Med. Chem. Lett.* **2009**, *19*, 3651.
- Hildmann, C.; Wegener, D.; Riester, D.; Hempel, R.; Schober, A.; Merana, J.; Giurato, L.; Guccione, S.; Nielsen, T. K.; Ficner, R.; Schwienhorst, A. *J. Biotechnol.* **2006**, *124*, 258.
- Takai, N.; Narahara, H. *J. Oncol.* **2010**, *2010*, 458431.
- Oger, F.; Lecorgne, A.; Sala, E.; Nardese, V.; Demay, F.; Chevance, S.; Desravines, D. C.; Aleksandrova, N.; Le, G. R.; Lorenzi, S.; Beccari, A. R.; Barath, P.; Hart, D. J.; Bondon, A.; Carettoni, D.; Simonneaux, G.; Salbert, G. *J. Med. Chem.* **2010**, *53*, 1937.
- Bressi, J. C.; Jennings, A. J.; Skene, R.; Wu, Y.; Melkus, R.; De, J. R.; O'Connell, S.; Grimshaw, C. E.; Navre, M.; Gangloff, A. R. *Bioorg. Med. Chem. Lett.* **2010**, *20*, 3142.
- Kiefer, F.; Arnold, K.; Kunzli, M.; Bordoli, L.; Schwede, T. *Nucleic Acids Res.* **2009**, *37*, D387–D392.
- Grosdidier, A.; Zoete, V.; Michielin, O. *Nucleic Acids Res.* **2011**, *39*, W270–W277.
- Hess, B.; Kutzner, C.; van der Spoel, D.; Lindahl, E. *J. Chem. Theory Comput.* **2008**, *4*, 435.
- DePaul, A. J.; Thompson, E. J.; Patel, S. S.; Haldeman, K.; Sorin, E. J. *Nucleic Acids Res.* **2010**, *38*, 4856.
- Jorgensen, W. L.; Madura, J. D. *Mol. Phys.* **1985**, *56*, 1381.
- Humphrey, W.; Dalke, A.; Schulten, K. *J. Mol. Graphics Modell.* **1996**, *14*, 33.
- Wegener, D.; Hildmann, C.; Riester, D.; Schwienhorst, A. *Anal. Biochem.* **2003**, *321*, 202.
- Cheng, Y.; Prusoff, W. H. *Biochem. Pharmacol.* **1973**, *22*, 3099.